Atmospheric carbon dioxide concentrations over the past 60 million years

Paul N. Pearson* **& Martin R. Palmer†**

** Department of Earth Sciences, University of Bristol, Queens Road, Bristol BS8 1RJ, UK*
† T. H. Huxley School, Imperial College, RSM Building, Prince Consort Road, London SW7 2BP, UK

Knowledge of the evolution of atmospheric carbon dioxide concentrations throughout the Earth's history is important for a reconstruction of the links between climate and radiative forcing of the Earth's surface temperatures. Although atmospheric carbon dioxide concentrations in the early Cenozoic era (about 60 Myr ago) are widely believed to have been higher than at present, there is disagreement regarding the exact carbon dioxide levels, the timing of the decline and the mechanisms that are most important for the control of CO_2 concentrations over geological timescales. Here we use the boron-isotope ratios of ancient planktonic foraminifer shells to estimate the pH of surface-layer sea water throughout the past 60 million years, which can be used to reconstruct atmospheric CO_2 concentrations. We estimate CO_2 concentrations of more than 2,000 p.p.m. for the late Palaeocene and earliest Eocene periods (from about 60 to 52 Myr ago), and find an erratic decline between 55 and 40 Myr ago that may have been caused by reduced CO_2 outgassing from ocean ridges, volcanoes and metamorphic belts and increased carbon burial. Since the early Miocene (about 24 Myr ago), atmospheric CO_2 concentrations appear to have remained below 500 p.p.m. and were more stable than before, although transient intervals of CO_2 reduction may have occurred during periods of rapid cooling approximately 15 and 3 Myr ago.

More than a century has passed since Arrhenius[1] proposed that early Cenozoic warmth was caused by high levels of carbon dioxide in the atmosphere and Chamberlin[2] suggested a variety of geological processes that could affect atmospheric carbon dioxide concentrations (p_{CO_2}). However, there is still disagreement as to the most significant controls on p_{CO_2} over long timescales. Some authors have stressed the importance of changing inputs to the atmosphere such as volcanic and hydrothermal outgassing[3,4] or metamorphic decarbonation reactions[5], while others have focused on outputs such as the weathering of silicate minerals and limestone formation[6–8] or organic carbon burial[9–11]. The level of early Cenozoic p_{CO_2} and when it might have declined is also still under debate[5–7,10,11].

The boron-isotope ($\delta^{11}B$) approach to p_{CO_2} estimation relies on the fact that a rise in the atmospheric concentration will mean that more CO_2 is dissolved in the surface ocean, causing a reduction in its pH. We are able to estimate the pH of ancient sea water by measuring the boron-isotope composition of calcium carbonate ($\delta^{11}B_{cc}$) precipitated from it. This is because boron in aqueous solution occurs as two species, $B(OH)_3$ and $B(OH)_4^-$, between which the equilibrium is strongly pH-dependent over the natural acidity range of sea water. Furthermore, there is a pronounced isotopic fractionation between the species of approximately −19.5‰, so that the $\delta^{11}B$ of each species is highly dependent[12] on pH. Because boron incorporation into marine carbonates is predominantly from $B(OH)_4^-$, $\delta^{11}B_{cc}$ is a sensitive pH indicator[13,14]. The pH of sea water is governed by the carbonate equilibria, such that for a given pH value it is possible to calculate the aqueous CO_2 concentration and thereby make quantitative estimates[15–20] of atmospheric p_{CO_2}.

The pH and aqueous CO_2 concentration of the surface ocean vary spatially because of factors such as deep-water upwelling, local productivity regimes and freshwater inflows. To arrive at pH estimates that most closely reflect atmospheric p_{CO_2}, it is necessary to measure the $\delta^{11}B$ of carbonates that were precipitated far from coastal influences and sources of upwelling. The ideal setting is in the low-latitude gyre systems, where a mixed layer of warm, low-density sea water in contact with the atmosphere generally overlies colder deep waters with little intermixing. Such environments support abundant planktonic foraminifera (a group of microscopic protists) that secrete calcite ($CaCO_3$) shells. The shells fall to the sea floor, from which a record of upper-ocean pH of many millions of years can be obtained.

We analysed the $\delta^{11}B$ of monospecific sample splits of surface mixed-layer dwelling foraminifera from 32 sediment samples from the open tropical Pacific, spanning the past 60 Myr, augmenting data from six other previously studied samples[19,20] (Table 1). It is necessary to use various species because none survived the entire time interval. Each monospecific sample consists of more than 100 individual shells that calcified at different times of the day and year over a period of several thousand years, so the small deviations from equilibrium pH and aqueous CO_2 that constantly occur in the upper ocean are likely to be averaged. Analytical methods were the same as previously published[19] and boron-isotope ratios are quoted relative to standard NBS SRM 951.

The study sites (Ocean Drilling Program Sites 865, 871 and 872) are all from the sedimentary caps of flat-topped seamounts in the tropical north Pacific gyre, and are characterized by exceptionally good carbonate preservation. They have been the subject of considerable previous geochemical work, including isotopic, trace element and microstructural characterization of the foraminifer shells[21–25]. There is no evidence from this work that diagenetic alteration has affected shell chemistry. We do not know of any similarly well preserved carbonates from the open ocean in the age range of 25–33 Myr ago.

In order for a pH value to be calculated from a $\delta^{11}B_{cc}$ measurement, it is necessary to assume a value for the boron-isotope composition of sea water ($\delta^{11}B_{sw}$); currently this value is +39.5‰, but it may have changed through time. Fortunately, geologically rapid fluctuations in $\delta^{11}B_{sw}$ are unlikely to have occurred as dissolved boron has a long residence time[26] in the ocean of approximately 20 Myr. We can estimate past $\delta^{11}B_{sw}$ values by utilizing the fact that different planktonic foraminifera species calcify from the surface mixed layer to the low pH conditions below the thermocline. The magnitude of the pH decline is controlled mainly by the local level of biological production, because

© 2000 Macmillan Magazines Ltd

more productive locations have a greater flux of sinking organic particles, which oxidize in the water column, reducing pH at depth. Although there is good evidence that the sites we analysed were always oligotrophic (with a maximum apparent oxygen utilization between 50 and 150 $\mu M\,kg^{-1}$), in six previously studied time windows in the Cenozoic we have observed substantial differences in the $\delta^{11}B_{cc}$ differential between surface and deep planktonic environments[19,20]. As we have argued[20], such differences can be explained as having been caused by variation in $\delta^{11}B_{sw}$. Hence, we use the value of the $\delta^{11}B_{cc}$ differential to model $\delta^{11}B_{sw}$ for each time window and interpolate $\delta^{11}B_{sw}$ values for the other samples (Table 1).

Changes in sea surface temperature (SST) also affect pH and p_{CO_2} estimates because the boric acid and carbonate equilibria are temperature dependent. However, oxygen isotopic studies have shown that the tropical SST has remained surprisingly constant through the Cenozoic despite pronounced cooling in the high latitudes[27]. We have assumed a SST of 27 °C for all our samples.

The $\delta^{11}B$ of surface-dwelling foraminifera may not provide a good estimate of pH in the mixed layer if the microenvironment of the foraminifer cell has a distinctive pH because of photosynthesis by algal symbionts. A symbiont "vital effect" on $\delta^{11}B_{cc}$ has been suggested for the analagous but much larger aragonitic skeletons of corals[28]. Microsensor studies of the living symbiotic species *Globigerinoides trilobus* (also known as *G. sacculifer*) and related taxa show that pH increases over short distances as the foraminifer shell is approached[29,30]. However, there is evidence that *G. trilobus* precipitates its shell with no boron-isotope vital effect[16–18]. Furthermore, because our analyses of various extinct species produces an oceanographically consistent pH–depth profile[20], we infer that Palaeogene surface-dwelling species of the genera *Acarinina* and *Morozovella* also precipitated their shells at or close to boron-isotopic equilibrium.

However, one of the species studied, upper Eocene *Hantkenina alabamensis*, yielded extremely negative $\delta^{11}B_{cc}$ values in all three samples analysed that cannot be interpreted using the pH model (see Table 1). As there is no textural or geochemical reason to suspect diagenetic alteration[25], we conclude that a strong vital effect fractionation of the boron isotopes occurred in this species. One possibility is that *H. alabamensis* (which has a very involute shell and large enveloping final chambers) resorbed earlier-formed calcite late in its life cycle, thereby reworking isotopically light boron. These data are excluded from subsequent geochemical calculations.

Figure 1 illustrates the record of sea surface pH that we have reconstructed from the $\delta^{11}B_{cc}$ data. Our finding that the pH was significantly lower in the early Palaeogene than in the Neogene period has implications for a wide range of biological and chemical processes in the ocean. For example, the speciation of a number of dissolved elements in sea water (such as P, N, Mn and Se) undergoes variations over the range of pH values (7.4–8.3) calculated in this study. The surface ocean would not have been so acidic as to inhibit biological calcification, but other more subtle effects on plankton ecology and sedimentation patterns may have occurred.

Reconstructing seawater carbon chemistry

The pH of the surface ocean is one of four key variables that define its carbonate chemistry, the others being the concentration of aqueous CO_2, the amount of total dissolved inorganic carbon (ΣCO_2) and the total alkalinity[31]. In order to calculate a value for p_{CO_2} it is necessary to assume a value for ΣCO_2 or alkalinity. Unfortunately, no reliable record of variations in either parameter

Table 1 Boron-isotope measurements of shallow-dwelling planktonic foraminifera and the calculated pH values

Age (Myr ago)	Top datum	Bottom datum	Hole	Sample (cm)	Species, size range (μm)	$\delta^{11}B_{cc}$	Analytical error (2σ)	$\delta^{11}B_{sw}$ model	pH
0.085	0.06	0.11	871A	1H/1, 124–126	Various	24.9	0.4	39.10	8.10
0.98	0.47	1.37	871A	2H/2, 59–61	*G. trilobus*, 500–600	25.1	0.1	39.10	8.12
1.49	1.45	1.68	871A	2H/6, 59–61	*G. trilobus*, 500–600	25.2	0.3	39.10	8.13
3.00	2.9	3.1	871A	3H/2, 123–125	Various	25.9	0.4	39.10	8.21
3.31	3.1	3.5	872C	3H/2, 59–61	*G. trilobus*, 500–600	25.5	0.1	39.03	8.17
3.87	3.8	3.9	872C	3H/5, 118–120	*G. trilobus*, 500–600	25.1	0.2	38.91	8.14
6.00	5.8	7.1	871A	3H/5, 60–62	*G. trilobus*, 500–600	24.9	0.1	38.59	8.15
6.20	5.8	7.1	871A	3H/5, 123–125	Various	24.5	0.3	38.53	8.12
9.02	7.1	10.2	872C	5H/2, 14–16	*G. trilobus*, 500–600	25.0	0.1	38.30	8.20
10.39	10.2	10.4	872C	5H/6, 59–61	*G. trilobus*, 500–600	24.5	0.2	37.99	8.18
11.40	11.3	11.5	872C	6H/5, 20–22	*G. trilobus*, 500–600	24.4	0.4	37.79	8.19
11.81	11.5	12.6	871A	4H/5, 59–61	Various	24.1	0.3	37.70	8.16
13.06	12.6	13.1	871A	6H/6, 60–62	*G. trilobus*, 300–425	24.4	0.4	37.70	8.20
14.73	14.6	14.9	871A	7H/2, 124–126	*G. trilobus*, 300–425	25.5	0.4	37.70	8.31
14.96	14.9	15.2	871A	7H/5, 59–61	*G. trilobus*, 300–425	25.0	0.2	37.70	8.26
16.23	16.2	16.3	871A	8H/2, 59–63	Various	23.7	0.4	37.70	8.14
16.70	16.6	19.0	872C	11H/1, 20–22	*G. trilobus*, 300–425	24.3	0.3	37.75	8.18
18.38	16.6	19.0	872C	11H/6, 20–22	*G. trilobus*, 300–425	24.6	0.1	37.84	8.20
19.85	19.0	21.8	872C	12H/2, 78–80	*G. trilobus*, 300–425	24.7	0.4	37.97	8.20
21.70	19.0	21.8	872C	13H/3, 20–22	*G. trilobus*, 300–425	24.7	0.4	38.03	8.19
23.00	22.8	23.2	872C	13H/5, 20–22	*G. trilobus*, 300–425	24.3	0.1	38.12	8.12
23.51	23.2	23.7	872C	14H/4, 20–22	*G. trilobus*, 300–425	23.5	0.2	38.19	8.04
34.84	34.0	35.2	865C	3H/5, 110–112	*H. alabamensis*, >250	11.0*			
36.10	35.2	38.4	865C	4H/1, 110–112	*H. alabamensis*, >250	11.4*			
39.51	38.4	40.1	865C	4H/5, 110–112	*H. alabamensis*, >250	13.5*			
40.12	40.1	40.5	865C	5H/1, 110–112	*A. topilensis*, 300–425	23.0	0.5	39.24	7.80
42.52	40.5	43.6	865C	6H/2, 65–67	Various	25.0	0.5	39.40	8.07
44.26	43.6	45.8	865C	7H/1, 110–112	*A. topilensis*, 300–425	24.1	0.2	39.40	7.95
45.69	43.6	45.8	865C	7H/3, 110–112	*A. praetopilensis*, 300–425	23.1	0.6	39.40	7.79
46.07	45.8	46.1	865C	8H/3, 110–112	*A. praetopilensis*, 300–425	22.0	0.1	39.40	7.54
46.97	46.1	49.0	865C	8H/5, 110–112	*A. praetopilensis*, 300–425	24.4	0.4	39.40	7.99
50.33	49.0	50.4	865C	9H/5, 110–112	*A. praetopilensis*, 500–600	23.4	0.1	39.40	7.84
51.02	50.8	52.3	865C	10H/1, 110–112	*M. caucasica*, 500–600	23.9	0.5	39.40	7.92
52.22	50.8	52.3	865C	10H/5, 100–102	*M. caucasica*, 425–500	21.6	0.2	39.40	7.42
53.24	52.3	54.0	865C	11H/1, 110–112	*M. marginodentata*, 425–500	22.3	0.4	39.40	7.62
55.84	54.7	55.9	865C	12H/5, 110–112	*M. velascoensis* s.l., 425–500	21.8	0.3	39.40	7.48
57.12	57.1	57.5	865C	14H/3, 110–112	*M. velascoensis* s.l., 300–425	22.0	0.4	39.40	7.54
59.88	59.2	60.0	865C	15H/5, 110–112	*M. velascoensis* s.l., 300–425	21.6	0.2	39.40	7.42

The ages of each sample were calculated by linear interpolation between reliable biostratigraphical datums for Sites 871 and 872 (as determined by ref. 50) and for Site 865 (R. D. Norris & H. Nishi, unpublished data). Samples consisting of various species are the means of analyses presented in previous studies[19,20]. Samples with an asterisk were exluded from subsequent geochemical calculations because they probably represent vital-effect fractionation of the boron isotopes. The $\delta^{11}B_{sw}$ value for each sample is calculated from the $\delta^{11}B_{sw}$ differential from surface to oxygen minimum zone at discrete levels, or interpolation between those levels following the method of ref. 20. *G.*, *Globigerinoides*; *H.*, *Hantkenina*; *A.*, *Acarinina*; *M.*, *Morozovella*.

© 2000 Macmillan Magazines Ltd

exists over the timescale covered by this study. However, variation in the carbonate compensation depth (CCD) in the ocean has previously been inferred from historical patterns of carbonate sedimentation[32], and this can be used to constrain alkalinity and ΣCO_2.

Our approach was to model the ancient ocean by adjusting alkalinity so as to ensure that the water column is exactly saturated with respect to calcite at the lysocline (which we take to be 500 m shallower than the CCD). The depth of the lysocline depends on the calcium concentration of sea water, $[Ca]_{sw}$, as well as the carbonate equilibria. The most important process that may have caused changes in $[Ca]_{sw}$ and alkalinity over the timescales considered in this study is variation in the river water flux. For example, continental weathering was probably more intense during periods of warm climate and high p_{CO_2}, which would deliver more Ca and HCO_3^- to the ocean. Therefore we have assumed that $[Ca]_{sw}$ has remained proportional to alkalinity. We then calculate surface-ocean alkalinity and ΣCO_2 by assuming that increases in these parameters with depth have remained the same as the modern western equatorial Pacific Ocean, that is, $\Delta\Sigma CO_2$ from 0 to 4,000 m equals 340 $\mu M\,kg^{-1}$, Δ(alkalinity) from 0 to 4,000 m equals 75 $\mu eq\,kg^{-1}$. Although this assumption may not be strictly correct, the relative homogeneity of sediment geochemistry in this area over the past 60 Myr (refs 21–24) means it has undergone considerably less variation in the factors that control depth variation in ΣCO_2 and alkalinity (principally productivity rates) than most other areas.

The calculated sea surface alkalinity record is shown in Fig. 2. The large amplitude variation in alkalinity over relatively short time periods in the Palaeogene is implied by the combined observations that the CCD was constant[32] but surface ocean pH varied markedly. However, we note that the CCD record for the Palaeogene Pacific Ocean is relatively poorly constrained, and it is possible that an updated study would imply less rapid alkalinity variation.

Having established values for surface ocean pH and alkalinity, it is possible to calculate aqueous CO_2 and atmospheric p_{CO_2}. The p_{CO_2} record is shown in Fig. 3a, with an expansion for the Neogene in Fig. 3b. We emphasize that the error bars in Figs 1 to 3 reflect only the analytical uncertainties in determining $\delta^{11}B_{cc}$. The absolute estimates must be treated with caution because there are other sources of error that are less easy to quantify. One important uncertainty is that the values of the various constants for carbonate equilibria in sea water have not been accurately measured at p_{CO_2} levels above 500 p.p.m. (ref. 33), and so are subject to revision. Other problems, as discussed above, include taking correct values for SST, $\delta^{11}B_{sw}$, $[Ca]_{sw}$, local biological productivity and CCD, as well as accounting for possible species-specific vital-effect fractionation and diagenetic alteration of the boron-isotope ratios. Despite these difficulties, which are similar to those encountered in other lines of palaeoclimate research, we believe that the timing and direction of the changes in the properties illustrated in Figs 1 to 3 are robust and warrant discussion.

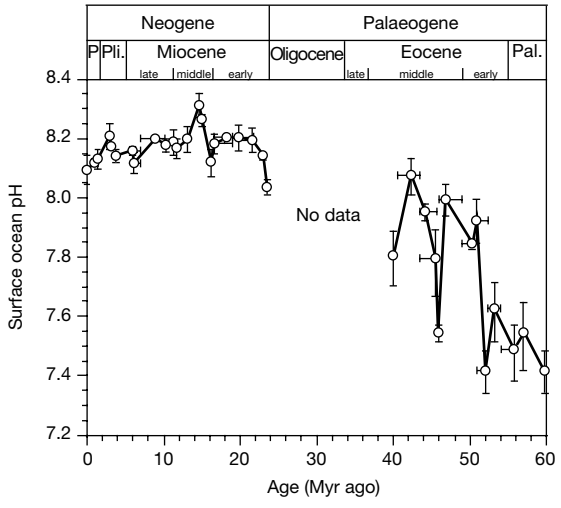

Figure 1 Sea surface pH for the past 60 Myr. Vertical error bars result from analytical error in determining $\delta^{11}B_{cc}$. Horizontal error bars represent the higher and lower biostratigraphical datums that constrain each sample (Table 1). Timescale according to ref. 49. P, Pleistocene; Pli., Pliocene; Pal., Palaeocene.

Causes of Cenozoic p_{CO_2} variation

Modelling of the atmosphere suggests that p_{CO_2} forces surface temperature in a logarithmic relationship. We use the equation of Kiehl and Dickinson[34] to estimate the level of greenhouse heating predicted by our p_{CO_2} estimates. We note that the relatively small changes in p_{CO_2} that occurred in the Neogene would have had a disproportionately large effect on surface temperature because absorption of outgoing radiation by CO_2 is further from saturation at low values. In Fig. 4, we compare this record with the oxygen-isotope ratio ($\delta^{18}O$) of deep sea benthic foraminifera[35–37], which is an important climate proxy that reflects both cooling and ice growth. Also indicated on Fig. 4 are some of the most important palaeoclimate events of the Cenozoic.

It has long been recognized that the early to early-middle Eocene (55 to 45 Myr ago) was a pivotal time in global climate evolution when a long-term cooling trend was initiated that ultimately resulted in the present glaciated Earth[38]. There is abundant geological evidence for large reorganizations of the carbon cycle in this interval. Our data indicate that a substantial reduction in p_{CO_2} occurred at this time, but the decline was not continuous, and the relationship with deep-sea temperature and ice growth was not straightforward.

During the late Palaeocene and early Eocene there was large-scale volcanic activity associated with North Atlantic rifting[39]. Enhanced volcanic outgassing of CO_2 may have been supplemented by magmatism and regional metamorphism in parts of the Himalayan belt[11] and North America[5]. Another source of CO_2 may have been the oxidation of methane released from storage either in wetlands[40] or from large seafloor gas hydrate reservoirs, as may have occurred in the short-lived Late Palaeocene thermal maximum event at 55 Myr ago[41] and similar subsequent events in the early Eocene[42]. In contrast, there is much less geological evidence for high levels of CO_2 emission in the later middle and upper Eocene.

We note that the termination of North Atlantic volcanism at about 54–53 Myr ago[40] corresponds approximately to the initial drop that we record in p_{CO_2} (Fig. 2). However, despite growing evidence for a short phase of cooling in the earliest Eocene[43], diverse geochemical and palaeontological indices suggest that the peak of

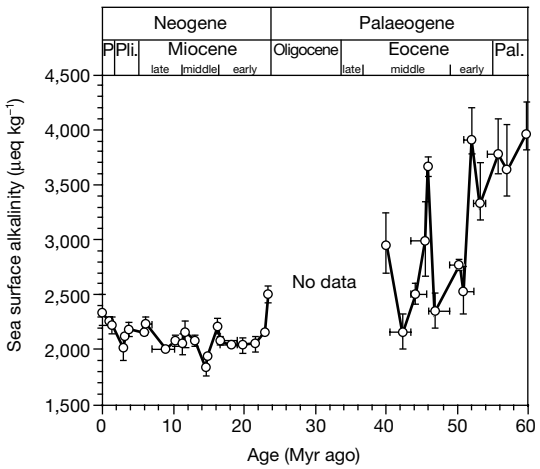

Figure 2 Sea surface alkalinity for the past 60 Myr. These values have been calculated by assuming that $[Ca]_{sw}$ has remained proportional to alkalinity. Epochs as for Fig. 1.

© 2000 Macmillan Magazines Ltd

global warmth was not reached until about 54–50 Myr ago[35–37], a time for which we estimate relatively lower p_{CO_2} values (700–900 p.p.m.). This was a period of maximum warmth and continental humidity combined with intermittently low sea level, causing extensive mangrove swamp and coal formation[10]. Deep weathering on the exposed continents may have accelerated the drawdown of CO_2. In addition, it has been proposed that continuing collision between India and Asia would have caused a progressive reduction in arc volcanism through this interval, combined with a switch from organic carbon (C_{org}) exhumation on the Indian continental shelf to C_{org} burial in large foreland basins, bringing about a reduction[11] in p_{CO_2}.

High-latitude cooling began at about the time of a sharp sea-level regression at 50 Myr ago that corresponds to a widespread hiatus in marine sediments[35–37]. This event is the first of four major steps[36] (as highlighted on Fig. 4) that punctuate the long-term history of Cenozoic cooling. McGowran[10] has proposed that a reverse greenhouse effect operated at that time, caused by high levels of siliceous plankton productivity in the oceans and correspondingly enhanced rates of marine C_{org} burial. Our data do not support a precise covariation of p_{CO_2} and temperature; indeed we record a p_{CO_2} peak during the cooling phase at approximately 45.5 Myr ago. Nevertheless a longer-term link between C_{org} burial and p_{CO_2} cannot be ruled out. We note that a major transition in Cenozoic $\delta^{34}S_{sw}$ occurred 55–45 Myr ago as would result from extended deposition of high levels of pyrite in anoxic marine sediments[44], and this interval corresponds to a general decline in p_{CO_2}.

Overall, the p_{CO_2} values for the early Cenozoic show considerably more variability than do the values for the late Cenozoic. This may be partly due to the magnification of errors that occurs at low pH values, but it may also reflect greater instability of the global carbon system during warm periods. The relative constancy of p_{CO_2} values in the later Cenozoic is circumstantial evidence that p_{CO_2} is stabilized by a homeostatic feedback mechanism involving the greenhouse effect[45]. This is because radiative forcing is amplified at low p_{CO_2}, hence small variations would be damped more efficiently by homeostasis.

Our oldest samples from this set indicate that there was a

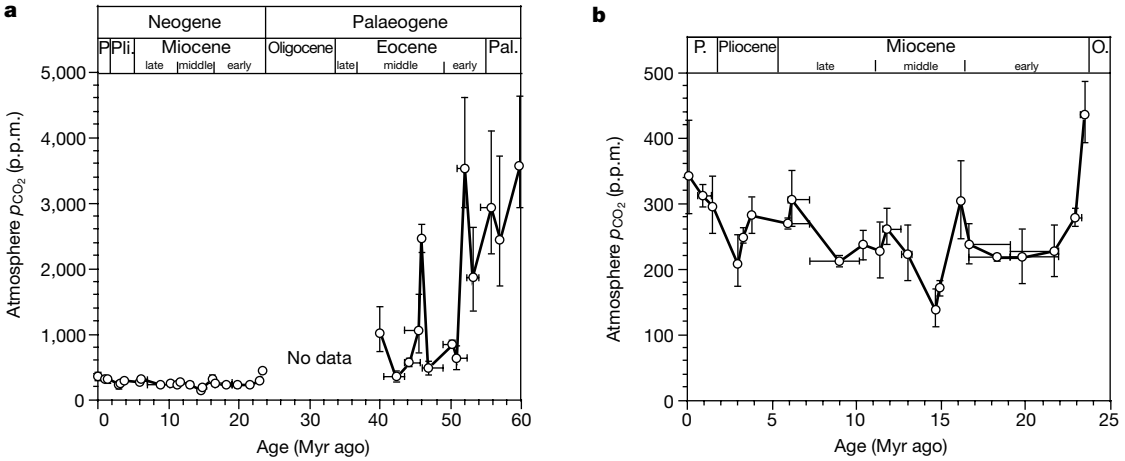

Figure 3 Record of atmospheric carbon dioxide for the past 60 Myr. **a**, The whole record; **b**, expansion for the past 25 Myr. We note that the nature of the pH–$\delta^{11}B_{cc}$ relationship means that analytical errors result in much larger uncertainties in the calculated p_{CO_2} at lower pH values. These values were calculated using a modified version of the carbonate equilibria presented in ref. 33. Epochs as for Fig. 1; O., Oligocene.

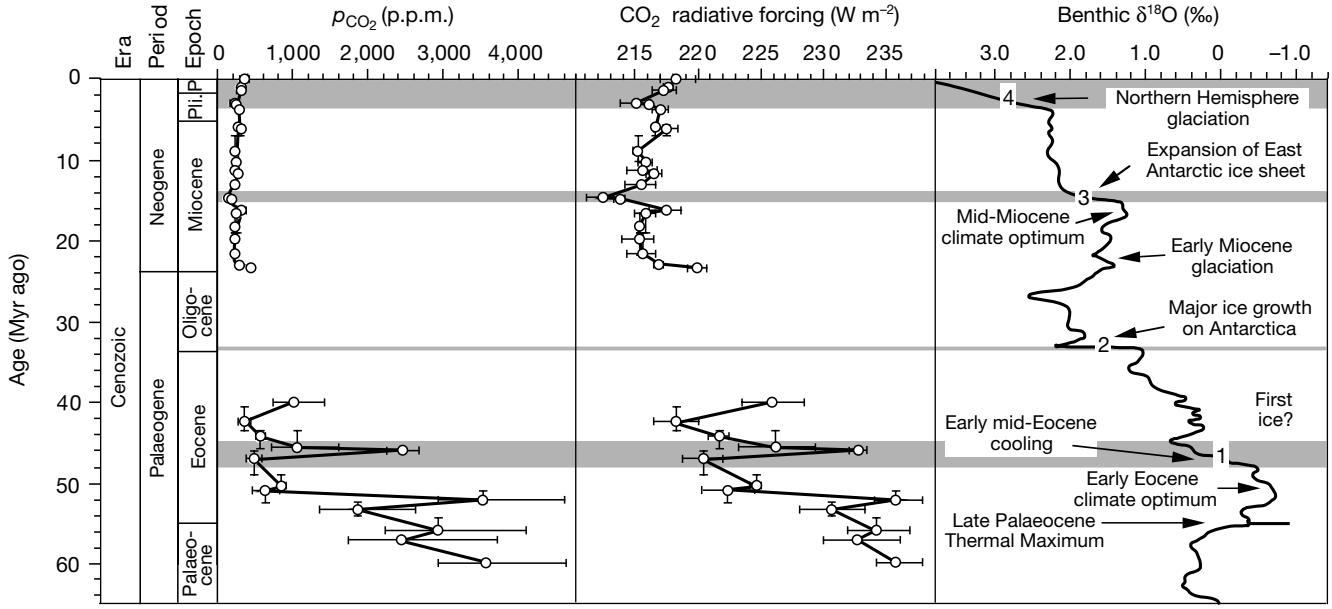

Figure 4 Carbon dioxide levels and Cenozoic climate change. The p_{CO_2} record is converted to radiative forcing (a measure of global warming) using the equation of Kiehl and Dickinson[34]. The benthic foraminifer $\delta^{18}O$ time series is a smoothed record of many observations summarized in refs 35–37. The trend towards more positive $\delta^{18}O$ results from a combination of deep-sea cooling and global ice volume increases. Four major steps (numbered 1 to 4) in $\delta^{18}O$ are indicated.

© 2000 Macmillan Magazines Ltd

reduction in p_{CO_2} in the lowermost Miocene. This was a time of high-latitude cooling that may have been associated with enhanced glaciation on Antarctica[36]. However, the most dramatic cooling phase in the Miocene was at 16–14 Myr ago, which has been interpreted as a major expansion of the East Antarctic Ice Sheet and increased formation of Antarctic Bottom Water[46]. This intensification of bottom-water formation would have been accompanied by accelerated upwelling of nutrient-rich water, which we would expect to have boosted productivity and caused a temporary reduction in atmospheric p_{CO_2}. A major increase in C_{org} burial in diatomites around the Pacific rim has been recorded at this time[9]. Our $\delta^{11}B_{cc}$ data suggest a transient p_{CO_2} decline from about 300 p.p.m. to 140 p.p.m. However, there is little support in our data (or the similar p_{CO_2} record produced recently[47] on the basis of biomarker carbon isotopes) for a large and permanent drop in p_{CO_2} during the middle Miocene, as has previously been suggested[8,9,15].

Another prominent step in the global cooling trend occurred in the late Pliocene (between about 4 and 2 Myr ago)[36] which culminated in the onset of major glaciation in the Northern Hemisphere. Once again, this step was probably associated with enhanced deep-water formation (this time in the North Atlantic), which would have led to a transient increase in surface-ocean productivity and a lowering of p_{CO_2}. We note a downturn in our p_{CO_2} record at this time, from about 280 to 210 p.p.m. Denser sampling will obviously be needed to test all these possible linkages.

Change in the carbon dioxide concentration of the atmosphere is commonly regarded as a likely forcing mechanism on global climate over geological time because of its large and predictable effect on temperature[48]. Our $\delta^{11}B_{cc}$ proxy for p_{CO_2} broadly confirms the prediction of Arrhenius[1] that early Cenozoic p_{CO_2} levels were often several times modern values, and that a strong greenhouse effect probably contributed to global warmth at that time. These 'super-greenhouse' conditions ($p_{CO_2} > 1{,}000$ p.p.m.) also imply considerably lower surface-ocean pH, higher alkalinity and higher levels of ΣCO_2. We find that there was considerable fluctuation in these variables in the Palaeogene, but since the earliest Miocene the system seems to have been much more constant and more closely comparable to the present, despite continuing climate cooling. This suggests that other factors, such as complex feedbacks initiated by tectonic alteration of the ocean basins, were also important in determining global climate change. □

Received 2 November 1999; accepted 22 June 2000.

1. Arrhenius, S. On the influence of carbonic acid in the air upon the temperature on the ground. *Phil. Mag.* **41,** 237–279 (1896).
2. Chamberlin, T. C. An attempt to frame a working hypothesis of the cause of glacial periods on an atmospheric basis. *J. Geol.* **7,** 545–584 (1898).
3. Owen, R. M. & Rea, D. K. Sea floor hydrothermal activity links climate to tectonics—the Eocene carbon dioxide greenhouse. *Science* **227,** 166–169 (1985).
4. Berner, R. A., Lasaga, A. C. & Garrels, R. M. The carbonate-silicate geochemical cycle and its effect on atmospheric carbon dioxide over the past 100 million years. *Am. J. Sci.* **283,** 641–683 (1993).
5. Kerrick, D. M. & Caldeira, K. Metamorphic CO_2 degassing from orogenic belts. *Chem. Geol.* **145,** 213–232 (1998).
6. Brady, P. V. The effect of silicate weathering on global temperature and atmospheric CO_2. *J. Geophys. Res.* **96,** 18101–18106 (1991).
7. Worsley, T. R., Moore, T. L., Fraticelli, C. M. & Scotese, C. R. Phanerozoic CO_2 levels and global temperatures inferred from changing paleogeography. *Geol. Soc. Am.* (Special Paper) **288,** 57–73 (1994).
8. Raymo, M. E. & Ruddiman, W. F. Tectonic forcing of late Cenozoic climate. *Nature* **359,** 117–122 (1992).
9. Berger, W. H. & Vincent, E. Deep-sea carbonates: reading the carbon-isotope signal. *Geologische Rundschau* **75,** 249–269 (1986).
10. McGowran, B. Silica burp in the Eocene ocean. *Geology* **17,** 857–860 (1989).
11. Beck, A., Sinha, A., Burbank, D. W., Seacombe, W. J. & Khan, S. in *Late Paleocene—Early Eocene Climatic and Biotic Events in the Marine and Terrestrial Records* (eds Aubry, M-P., Lucas, S. G. & Berggren, W. A.) 103–117 (Columbia Univ. Press, New York, 1998).
12. Kakihana, H., Kotaka, M., Satoh, S., Nomura, M. & Okamoto, M. Fundamental studies on the ion exchange separation of boron isotopes. *Bull. Chem. Soc. Jpn* **50,** 158–163 (1977).
13. Hemming, N. G. & Hanson, G. N. Boron isotope composition and concentration in modern marine carbonates. *Geochim. Cosmochim. Acta* **56,** 537–543 (1992).
14. Hemming, N. G., Reeder, R. J. & Hanson, G. N. Mineral-fluid partitioning and isotopic fractionation of boron in synthetic calcium carbonate. *Geochim. Cosmochim. Acta* **59,** 371–379 (1995).
15. Spivack, A. J., You, C. F. & Smith, H. J. Foraminiferal boron isotope ratios as a proxy for surface ocean pH over the past 21 Myr. *Nature* **363,** 149–151 (1993).
16. Sanyal, A., Hemming, N. G., Hanson, G. N. & Broecker, W. S. Evidence for a higher pH in the glacial ocean from boron isotopes in foraminifera. *Nature* **373,** 234–236 (1995).
17. Sanyal, A. *et al.* Oceanic pH control on the boron isotopic composition of foraminifera: evidence from culture experiments. *Paleoceanography* **11,** 513–517 (1996).
18. Sanyal, A., Hemming, N. G., Broecker, W. S. & Hanson, G. N. Changes in pH in the eastern equatorial Pacific across Stage 5-6 boundary based on boron isotopes in foraminifera. *Glob. Biogeochem. Cycles* **11,** 125–133 (1997).
19. Palmer, M. R., Pearson, P. N. & Cobb, S. J. Reconstructing past ocean pH-depth profiles. *Science* **282,** 1468–1471 (1998).
20. Pearson, P. N. & Palmer, M. R. Middle Eocene seawater pH and atmospheric carbon dioxide concentrations. *Science* **284,** 1824–1826 (1999).
21. Bralower, T. J. *et al.* Late Paleocene to Eocene paleoceanography of the equatorial Pacific Ocean: Stable isotopes recorded at Ocean Drilling Program Site 865, Allison Guyot. *Paleoceanography* **10,** 841–865 (1995).
22. Pearson, P. N. & Shackleton, N. J. Neogene multispecies planktonic foraminifer stable isotope record, Site 871, Limalok Guyot. *Proc. ODP Sci. Res.* **144,** 401–410 (1995).
23. Israelson, C., Buchardt, B., Haggerty, J. A. & Pearson, P. N. Carbonate and pore water geochemistry of pelagic caps at Limalok and Lo-En guyots, western Pacific. *Proc. ODP Sci. Res.* **144,** 737–743 (1995).
24. Opdyke, B. N. & Pearson, P. N. Geochemical analysis of multiple planktonic foraminifer species at discrete time intervals. *Proc. ODP Sci. Res.* **144,** 993–995 (1995).
25. Coxall, H. K., Pearson, P. N., Shackleton, N. J. & Hall, M. A. Hantkeninid depth adaptation: an evolving life-strategy in a changing ocean. *Geology* **28,** 87–90 (2000).
26. Taylor, S. R. & McLennan, S. M. *The Continental Crust: Its Composition and Evolution* (Blackwell Scientific, Oxford, 1985).
27. Zachos, J. C., Lohmann, K. C., Walker, J. C. G & Wise, S. W. Abrupt climate change and transient climates during the Paleogene: a marine perspective. *J. Geol.* **101,** 191–213 (1993).
28. Hemming, N. G., Guilderson, T. P. & Fairbanks, R. G. Seasonal variations in the boron isotopic composition of coral: A productivity signal? *Glob. Biogeochem. Cycles* **12,** 581–586 (1998).
29. Jorgensen, B. B. *et al.* Symbiotic photosynthesis in a planktonic foraminiferan, *Globigerinoides sacculifer* (Brady) studied with microelectrodes. *Limnol. Oceanogr.* **30,** 1253–1267 (1985).
30. Rink, S. *et al.* Microsensor studies of photosynthesis and respiration in the symbiotic foraminifer *Orbulina universa*. *Mar. Biol.* **131,** 583–595 (1998).
31. Millero, F. J. Thermodynamics of the carbon dioxide system in the oceans. *Geochim. Cosmochim. Acta* **59,** 661–677 (1995).
32. Van Andel, T. J. Mesozoic-Cenozoic calcite compensation depth and the global distribution of calcareous sediments. *Earth Planet. Sci. Lett.* **26,** 187–194 (1975).
33. Wanninkhof, R., Lewis, E., Feely, R. A. & Millero, F. J. The optimal carbonate dissociation constants for determining surface water p_{CO_2} from alkalinity and total inorganic carbon. *Mar. Chem.* **65,** 291–301 (1999).
34. Kiehl, J. T. & Dickinson, R. E. A study of the radiative effects of enhanced atmospheric CO_2 and CH_4 on early Earth surface temperatures. *J. Geophys. Res.* **92,** 2991–2998 (1987).
35. Shackleton, N. J. Palaeogene stable isotope events. *Palaeogeogr. Palaeoclimatol. Palaeoecol.* **57,** 91–102 (1986).
36. Miller, K. G., Fairbanks, R. G. & Mountain, G. S. Tertiary oxygen isotope synthesis, sea level history, and continental margin erosion. *Paleoceanography* **2,** 1–19 (1987).
37. Zachos, J. C., Stott, L. D. & Lohmann, K. C. Evolution of early Cenozoic temperatures. *Paleoceanography* **9,** 353–387 (1994).
38. Frakes, L. A., Francis, J. E. & Syktus, J. I. *Climate Modes of the Phanerozoic* (Cambridge Univ. Press, Cambridge, 1992).
39. Ritchie, J. D. & Hitchen, K. in *Correlation of the Early Paleogene in Northwest Europe* (eds Knox, R. W. O., Corfield, R. M. & Dunay, R. E.) 63–78 (Special Publication 101, Geological Society, 1996).
40. Sloan, L. C. *et al.* Possible methane-induced polar warming in the early Eocene. *Nature* **357,** 320–322 (1992).
41. Dickens, G. R., O'Neill, J. R., Rea, D. K. & Owen, R. M. Dissociation of oceanic methane hydrate as a cause of the carbon isotope excursion at the end of the Paleocene. *Paleoceanography* **10,** 965–971 (1995).
42. Thomas, E., Zachos, J. C. & Bralower, T. S. in *Warm Climates in Earth History* (eds Huber, B. T., MacLeod, K. S. & Wing, S. C.). 132–160 (Cambridge Univ. Press, Cambridge, 2000).
43. Wing, S. L., Bao, H. & Koch, P. L. in *Warm Climates in Earth History* (eds Huber, B. T., MacLeod, K. S. & Wing, S. C.). 197–237 (Cambridge Univ. Press, Cambridge, 2000).
44. Paytan, A., Kastner, M., Campbell, D. & Thiemens, M. H. Sulfur isotopic composition of Cenozoic seawater sulfate. *Science* **282,** 1459–1462 (1998).
45. Broecker, W. S. & Sanyal, A. Does atmospheric CO_2 police the rate of chemical weathering? *Glob. Biogeochem. Cycles* **12,** 403–408 (1998).
46. Wright, J. D., Miller, K. G. & Fairbanks, R. G. Early and middle Miocene stable isotopes; Implications for deepwater circulation and climate. *Paleoceanography* **7,** 357–389 (1992).
47. Pagani, M., Arthur, M. A. & Freeman, K. H. Miocene evolution of atmospheric carbon dioxide. *Paleoceanography* **14,** 273–292 (1999).
48. Crowley, T. J. in *Warm Climates in Earth History* (eds Huber, B. T., MacLeod, K. S. & Wing, S. C.). 425–444 (Cambridge Univ. Press, Cambridge, 2000).
49. Berggren, W. A., Kent, D. V., Swisher, C. C. & Aubry, M.-P. A revised Cenozoic geochronology and chronostratigraphy. 129–212 (Special Publication 54, Society of Economic Paleontologists and Mineralogists, 1995).
50. Pearson, P. N. Planktonic foraminifer biostratigraphy and the development of pelagic caps on guyots in the Marshall Islands group. *Proc. ODP Sci. Res.* **144,** 21–59 (1995).

Acknowledgements

The authors contributed equally to this work. Samples were provided by the Ocean Drilling Program. We thank S. Cobb for assistance in sample preparation. This work was supported by the Natural Environment Research Council. P.N.P. is supported by a Royal Society University Research Fellowship.

Correspondence and requests for materials should be addressed to P.N.P. (e-mail: Paul.Pearson@Bristol.ac.uk).

© 2000 Macmillan Magazines Ltd